Published in final edited form as:

SLAS Discov. 2017 February ; 22(2): 176–186. doi:10.1177/1087057116674312.

High-Throughput Screens to Discover Small-Molecule Modulators of Ryanodine Receptor Calcium Release Channels

Robyn T. Rebbeck[1], **Maram M. Essawy**[1], **Florentin R. Nitu**[1], **Benjamin D. Grant**[2], **Gregory D. Gillispie**[2], **David D. Thomas**[1], **Donald M. Bers**[3], and **Razvan L. Cornea**[1]

[1]Department of Biochemistry, Molecular Biology and Biophysics, University of Minnesota, USA

[2]Fluorescence Innovations, Inc., Minneapolis, MN, USA

[3]Department of Pharmacology, University of California, Davis, USA

Abstract

Using time-resolved fluorescence resonance energy transfer (FRET), we have developed and validated the first high-throughput screening (HTS) method to discover compounds that modulate an intracellular Ca^{2+} channel, the ryanodine receptor (RyR), for therapeutic applications. Intracellular Ca^{2+} regulation is critical for striated muscle function, and RyR is a central player. At resting [Ca^{2+}], increased propensity of channel opening due to RyR dysregulation is associated with severe cardiac and skeletal myopathies, diabetes and neurological disorders. This leaky state of the RyR is an attractive target for pharmacological agents to treat such pathologies. Our FRET-based HTS detects RyR binding of accessory proteins calmodulin or FKBP12.6. Under conditions that mimic a pathological state, we carried out a screen of the 727-compound NIH Clinical Collection, which yielded six compounds that reproducibly changed FRET by >3SD. Dose-response of FRET and [^{3}H]ryanodine binding readouts reveal that five hits reproducibly alter RyR1 structure and activity. One compound increased FRET and inhibited RyR1, which was only significant at nM [Ca^{2+}], and accentuated without CaM present. These properties characterize a compound that could mitigate RyR1 leak. An excellent z′-factor and the tight correlation between structural and functional readouts validate this first HTS method to identify RyR modulators.

Keywords

calcium channel; RyR; sarco/endoplasmic reticulum; fluorescence lifetime; calcium leak

INTRODUCTION

Embedded in the sarcoplasmic reticulum (SR) membrane of striated muscle, ryanodine receptors (RyR) are responsible for intracellular Ca^{2+} release that triggers muscle contraction. Dysregulation of skeletal (RyR1) and cardiac (RyR2) isoforms is implicated in

Corresponding Author: Razvan L. Cornea, Department of Biochemistry, Molecular Biology and Biophysics, University of Minnesota, 321 Church Street SE, Minneapolis, MN 55455. Phone: +1-612-626-2660, corne002@umn.edu.

DECLARATION OF CONFLICTING INTERESTS

DDT and RLC hold equity in, and serve as executive officers for Photonic Pharma LLC. These relationships have been reviewed and managed by the University of Minnesota. Photonic Pharma had no role in this study.

the pathology of severe diseases, including malignant hyperthermia (MH), central core disease (CCD), muscular dystrophy, sarcopenia, heart failure (HF), diabetes, Alzheimer's disease (AD) (1–5). In most of these cases, pathogenesis is, in part, attributed to excess SR Ca^{2+} "leak" via RyR under resting cellular conditions, and thus RyR is an intensely studied therapeutic target. Indeed, there are RyR small-molecule modulators that have been identified as possible therapeutic agents, including dantrolene, flecainide, tetracaine, K201, and S44121. However, most of these candidate drugs are known to also deleteriously interact with and functionally modulate other targets, and thus have side-effects that render them unsuitable for chronic therapeutic use (6,7). Certainly, a large expansion in the list of RyR regulators would greatly benefit the advancement of RyR-targeted pharmaceutical approaches to treating several skeletal and cardiac myopathies.

The RyR is tightly regulated by endogenous proteins, such as calmodulin (CaM) and FK-506 binding proteins (FKBP) 12.0 and 12.6, that are associated with maintaining normal Ca^{2+} cycling (8). Binding of CaM and FKBP to RyR has been shown to be sensitive to small-molecule RyR modulators (dantrolene, K201 and S44121) and RyR posttranslational modifications (9–12). Despite some controversy regarding the correlation between RyR phosphorylation and FKBP association (8), the collective of studies indicate that CaM, and possibly also FKBP, binding to RyR may be used as sensitive indicators of the RyR structural state associated with Ca leak (11–15).

Ideally, at the foundation of a target-directed high-throughput screen (HTS) is an effective method of monitoring the target's activity that can be adapted for high-throughput measurement. As of yet, a true RyR-directed HTS method has not been reported, which may be attributed to the low-throughput nature of the methods that are currently used to directly assess RyR activity. Thus, a method that detects a signal that correlates with RyR function and is truly measurable in a high throughput manner is highly desirable for identifying drug-like RyR modulators within libraries of small-molecule compounds. In this study, we aimed to validate an HTS-compatible method of seeking small-molecule modulators of RyR using time-resolved fluorescence resonance energy transfer (TR-FRET) as readout for a structural change in RyR1 or a shift in levels of CaM or FKBP binding. Our established molecular toolkit, as shown in Figure 1A, involves measuring FRET between an excited donor fluorophore attached to a single-Cys FKBP12.6 (D-FKBP) and an acceptor fluorophore attached to a single-Cys CaM (A-CaM), when both of these fluorescently labeled proteins are bound to RyR in native SR membranes (17,18). When A-CaM is bound to RyR in the proximity of D-FKBP, FRET is measured as a decrease in donor fluorophore fluorescence intensity (17) or fluorescence lifetime (FLT, calculated from the TR-fluorescence decay waveforms; Figure 1B). Changes in FRET due to an RyR modulator reflect changes in FKBP and/or CaM binding, and/or in RyR structure, as shown in Figure 1C. We integrated this FRET-based molecular toolkit that targets RyRs with the use of an FLT plate-reader (FLT-PR) (19,20) to undertake a duplicate screen of the 727-compound NIH clinical collection (NCC). Using this technology, a high-precision (S/N>100) TR-fluorescence decay, averaged from 200 fluorescence waveforms is read in 200 ms, and a whole 384-well plate is scanned within 3 min. In this screen we identified six compounds that reproducibly altered FRET in duplicate runs. Five of these compounds also reproducibly altered FRET in dose-response assays, and all of these compounds altered RyR1 activity, as measured by

[^{3}H]ryanodine binding, in a fashion that typically inversely correlated with the shift in FRET. Therefore, we present an HTS assay to detect both activators and inhibitors of the RyR, and thus validated a HTS-capable method that will be used to identify compounds of high therapeutic potential.

MATERIALS AND METHODS

The 727-compound NCC was purchased from Evotec (Hamburg, Germany) as 10-mM solutions in DMSO. The pig skeletal muscle (*longissimus dorsi*) was processed and purchased from Pel-Freez Biologicals (AR, USA). Fluorophores Alexa Fluor 488 C5-maleimide (AF488) and Alexa Fluor 568 C5-maleimide (AF568) were purchased from Life Technologies (OR, USA). Individual NCC compounds of interest (hits) were purchased separately, as following: disulfiram and ebselen from Fisher Scientific; chloroxine, diazoxide and fluphenazine from Sigma-Aldrich; cefatrizine propylene glycol (PG), and cefixime trihydrate and tacrolimus from Sequoia Research Products Ltd (Pangbourne, UK); and pravastatin and lofepramine from Santa Cruz Biotechnology (CA, USA).

Compound handling and preparation of 384-well assay plates

The NCC compounds were received in 96-well plates and reformatted into 384-well polypropylene intermediate plates (Greiner Bio-One, Kremsmunster, Austria) using a multichannel liquid handler, BioMek FX (Beckman Coulter, Miami, FL, USA), then transferred to 384-well Echo Qualified source-plates (Labcyte Inc, Sunnyvale, CA, USA). Assay plates were prepared by transferring 50 nL of the 10-mM compound stocks or DMSO from the source plates to 384-well black polypropylene plates (Greiner), using an Echo 550 acoustic dispenser (Labcyte Inc.). NCC compounds were formatted in three plates, with the first two and last two columns loaded with 50 nL of DMSO and used for drug-free controls. These assay plates were then heat-sealed using a PlateLoc Thermal Microplate Sealer (Agilent Tech., Santa Clara, CA, USA) and stored at −20ºC prior to usage.

Isolation of sarcoplasmic reticulum vesicles

SR membrane vesicles were isolated from pig *longissimus dorsi* muscle by differential centrifugation of homogenized tissue, in accordance with (21). Heavy SR (HSR) vesicles, which are enriched in RyR1, were isolated by fractionation of crude skeletal SR vesicles using a discontinuous sucrose gradient (21). All vesicles were flash-frozen and stored at −80ºC. Immediately prior to the fluorescence or [^{3}H]ryanodine binding studies described below, the SR vesicles were stripped of residual endogenous CaM by incubation with a peptide derived from CaM binding domain of myosin light chain kinase, followed by sedimentation, in accordance with (22).

Expression, purification and labeling of FKBP and CaM

Single-cysteine mutants of FKBP12.6 (C22A/R49C/C76I) and CaM (T34C) were expressed in *Escherichia coli* BL21(DE3)pLysS (Agilent Technologies, CA, USA), purified and were respectively labeled with fluorescent probes AF488 or AF568 as described previously (18,23). Stoichiometric labeling of FKBP and CaM with fluorescent probes to ≥95% was indicated by comparing the molar concentration of bound dye (determined from its

absorbance) to the protein concentration which was determined via a bicinchoninic-acid assay, (Thermo Fisher Scientific, Rockford IL) and SDS-PAGE densitometry. Essentially complete labeling was confirmed by electrospray ionization mass spectrometry. We have previously demonstrated that our system of donor-labeling FKBP12.6 (D-FKBP) with AF488 and acceptor labeling CaM(A-CaM) with AF568 does neither alter the endogenous binding nor modulatory activity of these RyR accessory proteins (17,18).

Preparation of SR vesicles for FRET measurement

HSR (0.4 mg/ml) membranes were pre-incubated with 60 nM D-FKBP, for 90 min, at 37ºC, in a solution containing 150 mM KCl, 5 mM GSH, 0.1 mg/mL BSA, 1μg/mL Aprotinin/Leupeptin, 1 mM DTT and 20 mM PIPES (pH 7.0). To remove unbound D-FKBP, the SR membranes were spun down at 110,000 × *g* for 20 min, and then resuspended to 1 mg/mL in binding buffer consisting of 150 mM KCl, 5 mM GSSG, 0.1 mg/mL BSA, 1μg/mL Aprotinin/Leupeptin and 20 mM PIPES, pH 7.0. These samples were then incubated with 0.3 μM A-CaM for 30 min at 22ºC in binding buffer containing 0.065 mM $CaCl_2$ to give 30 nM Ca^{2+} in the presence of 1 mM EGTA (calculated by MaxChelator). This labeled SR sample was applied to the NCC assay plates in 50 μL aliquots using a Multidrop™ Combi reagent dispenser (Thermo Scientific) with a standard-tube cassette that loaded a single plate within 30 sec. An additional set of the NCC assay plates were loaded with HSR labeled with only D-FKBP, not A-CaM.

Fluorescence data acquisition

Fluorescence lifetime measurements were conducted in a prototype top-read FLT-PR designed and built by Fluorescence Innovations, Inc., which reads each 384-well plate in ~3 minutes. AF488 donor fluorescence was excited with a 473-nm microchip laser from Concepts Research Corporation (Belgium, WI), and emission was acquired with 490-nm long-pass and 520/17-nm band-pass filters (Semrock, Rochester, NY). This instrument uses a unique direct waveform recording technology that enables high-throughput fluorescence lifetime detection at high precision (24). We have previously demonstrated the performance of this plate reader with known fluorescence standards, as well as with a FRET-based HTS method that targets SERCA (19,20).

HTS data analysis

TR-fluorescence waveforms for each well were fitted based on a two-exponential decay function using least-squares minimization global-analysis software (Fluorescence Innovations, Inc.). As indicated, the FRET efficiency (*E*) was determined as the fractional decrease of donor fluorescence lifetime (τ_D), due to the presence of acceptor fluorophore (τ_{DA}), using the following equation:

$$E = 1 - \frac{\tau_{DA}}{\tau_D}, \quad \text{Eq. (1)}$$

Assay quality was determined based on controls (DMSO-only samples) on each plate, as indexed by the Z′ factor (25):

$$Z' = 1 - 3\left(\frac{\sigma_D + \sigma_{DA}}{\mu_D - \mu_{DA}}\right) \quad \text{Eq. (2)}$$

where σ_D and σ_{DA} are the SDs of the control τ_D and τ_{DA}, respectively; μ_D and μ_{DA} are the means of the control τ_D and τ_{DA}, respectively. The Z' for the fluorescence peak data was calculated using Eq. (2) with σ_D and μ_D of control F_D, and, σ_{DA} and μ_{DA} of F_{DA}, based on controls present in each plate. A compound was considered a hit if it changed *E* by >3SD relative to that of control samples (E_0) that were exposed to 0.1% DMSO. The 3SD hit-selection threshold is typical for normally distributed HTS data, whereby 0.27% of the readings are expected to fall outside this limit. The threshold may be further adjusted to constrain the number of hits according to the resources available for evaluation via secondary (orthogonal) assays.

[^{3}H]ryanodine binding to SR vesicles—Skeletal SR membranes (1 mg/ml) were pre-incubated with 0.02% DMSO or hit compound, with or without 800 nM CaM, for 30 min at 4°C in a solution containing 150 mM KCl, 5 mM GSSG, 1 μg/mL Aprotinin/Leupeptin, 1 mM EGTA, and 65 μM or 1.02 mM $CaCl_2$ (as determined by MaxChelator to yield 30 nM or 30 μM Ca^{2+}, respectively), 0.1 mg/mL of BSA and 20 mM K-PIPES (pH 7.0). Non-specific and maximal [^{3}H]ryanodine binding to SR were separately assessed by addition of 20 μM non-radioactively labeled ryanodine or 5 mM Adenylyl-imidodiphosphate, respectively. Binding of [^{3}H]ryanodine (15 nM) was determined following a 3-h incubation at 37°C and filtration through grade GF/B Glass Microfiber filters (Brandel Inc., Gaithersburg, MD, US) using a Brandel Harvester. In 4 mL of Ecolite Scintillation cocktail (MP biomedicals, Solon, OH, USA), [^{3}H] on filter was counted using a Beckman LS6000 scintillation counter (Fullerton, CA).

RESULTS

HTS Performance

To validate the performance of our FRET-based HTS method for identification of novel RyR1 modulators that may have therapeutic benefit, we screened the NIH clinical collection (NCC), which is a 727-compound library of small molecules that have a history of use in human clinical trials. This diverse collection of small molecules is ideal for a pilot screen, particularly given that some molecules are known RyR modulators, such as dantrolene, tacrolimus and ebselen. The complete NCC was applied to columns 3–22 of three 384-well black-wall/black-bottom Greiner plates (drug-containing wells). Plate columns 1–2 and 23–24 were loaded with 50 nL of DMSO (and these wells were used for drug-free controls), using an Echo 550 acoustic dispenser (Labcyte Inc.). For each screen, one set of plates was loaded with D-FKBP labeled SR membranes (donor-only sample), while the other set was loaded with the D-FKBP labeled SR that was additionally incubated with 0.3 μM A-CaM (donor-acceptor sample) for 30 min prior to loading on the plates. This sub-saturating concentration of A-CaM was chosen to provide a readout that is sensitive to library compounds that may increase or decrease CaM binding to RyR. Final assay conditions also included 30 nM Ca^{2+} to represent resting [Ca^{2+}], and 5 mM oxidized glutathione (GSSG),

which exaggerates the conditions associated with oxidative stress (26). With these conditions, the objective was to promote a homogenous population of RyR1 that are associated with muscle pathologies. This is with a future goal of identifying RyR-targeted therapeutics for SR Ca^{2+} leak. These biological samples were loaded using a Multidrop Combi automated sample dispenser, as described above in the Materials and Methods.

TR-fluorescence decay waveforms were read in the FLT-PR over a time course of 5, 20, 40, 60 and 120 minutes after applying the SR sample to the assay plates. Although some compounds (chloroxine and ebselen) substantially altered FRET by the 20 min time point, the effect of small molecules that altered FRET was greatest or had plateaued by the 2-hour time point (Figure S1). Consequently, all results shown from here onwards refer to the 2-hour time-point. This behavior was not surprising given the very slow and moderate dissociation kinetics of FKBP12.6 and CaM, respectively, at 23–25ºC from RyR1 (17,27), and time necessary for potential oxidation-mediated effects. Fluorescence intensity values were measured from the peak values of the fluorescence decays in Figure 2A. The high coefficient of variance (CV) for the intensity measurement is quite apparent as differences between time-resolved fluorescence waveforms (Figure 2A). This fluorescence intensity readout produced a ~30× larger coefficient of variance (CV) relative to that of the fluorescence lifetime readout (time-resolved) (Figure 2B). This translates to excellent HTS assay quality when using fluorescence lifetime, and marginal reliability when using fluorescence intensity (Figure 2C). The increased reliability that is enabled by the lifetime measurement indicates an excellent HTS assay quality $Z' = 0.89 \pm 0.01$, which has been previously demonstrated in SERCA-based HTS (19). Therefore, we analyzed our NCC HTS FRET data based on the fluorescence lifetime readout. To set a threshold for “hit” compounds, we investigated the reproducibility of the compounds between duplicates of the screens with thresholds set at 1, 2, 3 and 4 standard deviations (SD) from the mean (Table S1). An acceptable hit rate for an HTS assay is ~0.5 to 3%, in order to yield a manageable load of post-HTS testing via orthogonal assays (28). Application of this guideline to our assay indicates that a threshold of 3SD would be suitable given the ~2% hit rate. Furthermore, this threshold results in the greatest yield of reproducible compounds between Screen 1 and Screen 2 (Table S1). Note that fluorescent test-compounds that interfere to produce FRET artifacts were flagged in donor-only plates by virtue of altering donor only sample lifetimes (τ_D) by >3SD relative to the DMSO controls. For the same purpose, we also read the fluorescence spectra of donor-only plates in a SpectraMax Gemini EM plate reader (Molecular Devices).

The overall effects on FRET, expressed as E/E_0, are shown in Figure 3A, but with the readouts from fluorescent compounds excluded. Of 14 and 16 hits from each screen (based on the (+) or (−) 3SD criterion), only 6 were reproducible, shown in Table S1. The ensemble of E/E_0 values fit well to a narrow Gaussian distribution ($\sigma = 0.02$) centered over the control mean ($\mu = 1.002$) (Figure 3B). We observed a skewed distribution of the hit compound effects, wherein only one compound increased FRET and five compounds decreased FRET (Figure 3C). These six hit compounds were further tested in dose-response FRET assays.

FRET Dose-Response Assays

Using the same assay condition as in the screens, we tested the dependence of FRET on the concentration of the reproducible hits (0.01–100 μM compound). We examined the effect of hits under Ca^{2+} conditions corresponding to muscle relaxation and contraction (30 nM or 30 μM free Ca^{2+}, respectively). The effect of the compounds largely replicated the effect observed in the screens, with one exception, Cefixime (Figure 4A), which was not further examined in functional studies. As a minor variation, disulfiram and cefatrizine were both found to decrease FRET in the screen, but increased FRET at 10 μM in the follow up dose response assays. However, both disulfiram and cefatrizine biphasically affected FRET, with exposure to >20 μM compound decreasing FRET in a manner consistent with the HTS readout (Figure 4A).

Given the role of tacrolimus (also known as FK506) in blocking both FKBP12 and FKBP12.6 from binding to RyRs (29), we were pleased that our primary screen identified this compound as a significant inhibitor of FRET at both 30 nM and 30 μM Ca^{2+} (Figure 4). Similarly, ebselen is another known RyR modulator, which has been shown to affect RyR1 activity, in a biphasic manner, via oxidation of RyR1 free thiols (30). However, ebselen has not been previously reported to perturb CaM or FKBP12.6 binding to RyR. Of the known RyR modulators present in NCC, we did not observe an effect of 10 μM dantrolene on FRET with skeletal SR, under these particular experimental conditions. This is consistent with previous reports that dantrolene does not alter CaM binding affinity to RyR1 in porcine skeletal SR membranes (31).

Disulfiram has been shown to increase Ca^{2+} uptake by SR in saponin-permeabilized rat skeletal muscle fibers without modulating caffeine sensitivity of Ca^{2+} release (32), thus suggesting that it did not act on the RyR. Yet, we observed an interesting biphasic effect of disulfiram on FRET at 30 nM Ca^{2+} – increased at 1–10 μM, and decreased at 20–100 μM compound (Figure 4A). Although this effect is greatly attenuated at 30 μM Ca^{2+} (Figure 4B).

Both cefatrizine and chloroxine are utilized therapeutically for their anti-bacterial properties, but neither drug has been reported, to date, to alter RyR activity or cellular Ca^{2+} homeostasis. As shown in Figure 4, chloroxine slightly increased FRET ($\Delta E \approx 0.05$) at ≥ 10 μM at 30 nM Ca^{2+}, but this effect is reversed to an inhibition of FRET in 30 μM Ca^{2+}. Similar to the effects of disulfiram, a biphasic effect was observable with Cefatrizine (Figure 4A), which also decreased FRET > 20 μM, consistent with the effect we observed in HTS mode. Furthermore, at 30 μM Ca^{2+}, we observed only a small FRET decrease (rather than a biphasic effect) at >20 μM Cefatrizine (Figure 4B).

Overall, the dose-response data confirms that five of the six hits modulate FRET, even a compound (chloroxine) with a very small effect on FRET ($\Delta E \approx 0.02$). The reproducibility of these compounds at 10 μM is high, as evidenced by the low CV (ranging from 0.5–4.1%).

Effect of Hits on RyR1 activity, as determined using [^{3}H]ryanodine binding to HSR

To evaluate the ability of our structure-based screen to identify functional modulators of RyR, we used [^{3}H]ryanodine binding to SR. The level of [^{3}H]ryanodine binding is a well-

established index of the channel activity in an RyR population, as presented in native SR membranes (23). Furthermore, this technique enables assay experimental conditions to be similar between RyR activity and FRET experiments. To determine whether a correlation exists between the FRET readout and RyR activity, we used the same overall experimental conditions in both types of assay.

Since CaM is a potent regulator of RyR activity and A-CaM was used in the FRET (structural) component of this study, we sought to determine whether CaM influences the functional effects of the hits. Thus, we carried out the [^{3}H]ryanodine binding measurements in the absence and presence of CaM (800 nM), over the same range of hit concentrations as in the FRET dose-response studies above (Figure 4). In accord with the well-established functional effect of CaM on RyR1, addition of CaM increased activity ([^{3}H]ryanodine binding) by ~4-fold in nM Ca^{2+}, and inhibited activity by ~70% in μM Ca^{2+} (Figure 5A). This response to a well-established RyR modulator indicates that our experimental conditions are adequate to detect functional effects by hits. Overall, relative to the matched DMSO controls, each compound modulated RyR1 activity in a Ca^{2+} dependent manner (Figure 5B–F). All compounds had the strongest effect on RyR1 activity at 30 nM Ca^{2+} and in the absence of CaM, strongly indicating that CaM binding RyR1 is not required for these compounds to affect RyR1 function.

At 30 nM Ca^{2+}, cefatrizine, disulfiram, ebselen, tacrolimus significantly increased RyR1 activity, whereas chloroxine inhibited it. For all compounds, the amplitudes of these effects were significantly reduced when CaM (800 nM) was present in the sample.

At 30 μM Ca^{2+}, the effects of all compounds were smaller and CaM influenced them in a less consistent manner than in 30 nM Ca^{2+}. Namely, CaM increased: the effects of cefatrizine and ebselen, did not significantly change those of disulfiram and tacrolimus, and changed that of chloroxine from slight inhibition to a biphasic profile peaking in a ~20% activation at 10 μM compound, then turning into inhibition at the higher μM concentrations tested.

For the purpose of identifying RyR modulators, dantrolene is a false negative in our method's readout. For a broader estimation of the rate of false negatives, we randomly selected a few non-reproducible hits (pravastatin, diazoxide, flufenazine, lofepramine) and found that, at 10 μM, they have no significant effect on RyR1 activity, as indicated by [^{3}H]ryanodine binding assays (Figure 5G). This assessment also suggests that there is a moderate rate of false positives in one screen, but this is much lower in duplicate screens. Overall, all of the compounds yielded by HTS as hits that were confirmed as FRET effectors in follow up dose response assays were found to functionally modulate RyR1. Though, the presence of CaM in 30 nM Ca^{2+} strongly impacts the functional effect of hits.

DISCUSSION

Excess SR Ca^{2+} leak under resting intracellular conditions is implicated in the pathology of several severe cardiac and skeletal myopathies, diabetes and neurological disorders. The dysregulation of RyR that promotes this leaky state of the channel is not only associated

with disease causing mutations in RyR, but also altered post-translational modifications that have been implicated in altering binding of RyR stabilizers, CaM and FKBP12/12.6 (1,3,4,6,10–12). Moreover, excessive post-translational modifications are typically thought as key players in late-stage pathology. Therefore, the pursuit of RyR-directed treatment agents is expected to produce clinically relevant outcomes – given the general appreciation in the field, based on compelling experimental evidence – that targeting RyR-mediated Ca^{2+} leak is effective for treating animal and cellular models of sarcopenia, muscular dystrophy, or arrhythmias (4,33). Ultimately, identification or design of novel small molecules that inhibit RyRs under resting (nanomolar [Ca^{2+}]) conditions is highly desirable in the pursuit of RyR-targeted therapeutics of myopathies. As of yet, however, advancement of RyR-targeted therapies, particularly pharmaceutical, is arrested by the lack of high-throughput methodologies to identify RyR modulators. We report on a key first step to address this important unmet clinical need.

To discover compounds that modulate RyR1, we adapted our well-established FRET system for rapid screen of a 727-compound library (NCC). By using fluorescence lifetime analysis of decay waveforms, we were able to identify even subtle changes of FRET, which could reflect a shift in the binding of CaM or FKBP to RyR, or a structural change in the RyR structure (Figure 1). With a threshold of 3SD of the mean, modulators that altered the FRET efficiency > 0.03 were considered hits. From follow-up FRET dose-response assays of the individually purchased compounds, we found that five of the screen hit compounds significantly altered FRET, albeit >20 μM of disulfiram and cefatrizine were necessary to produce the same reduction in FRET that was produced by 10 μM compound in the screen. The probable reason for these differences is variable compound degradation or their effective concentration in the source library. Based on this small screen, the apparent rate of false positives is 16%, which indicates that the 3SD hit-selection threshold is economically tenable.

The validity of our FRET readout as an indicator of RyR1 functional modulation is strongly supported by the observation that all five compounds that altered FRET in the dose-response assays also modulated RyR activity, as measured using [^{3}H]ryanodine binding assays. Thus, we have found that most hits reproducibly identified via HTS – i.e., using a structural readout – do also have a functional effect on RyR1. Particularly encouraging is the finding that one reproducible HTS hit that increased FRET (chloroxine) inhibited RyR1 function (as indicated by [^{3}H]ryanodine binding, Figure 5F), and this effect was largest under nM [Ca^{2+}] (resting) in the absence of CaM. These are the properties that we expect – at the stage of initial secondary studies following HTS – to characterize a compound that is likely to mitigate RyR1 leak *in situ*.

We compared ΔFRET to Δactivity for four different concentrations of each hit (≤ 20 μM), under nanomolar and micromolar Ca^{2+} (Figure 6A). As indicated by the slope of the linear fit (Figure 6B), most of the hits affect FRET and RyR activity in an inverse manner. That is, an increase in FRET is correlated with inhibition of [^{3}H]ryanodine binding (the effect we seek in a leak inhibitor), and a decrease in FRET correlates with increased [^{3}H]ryanodine binding (an effect indicative of potentially deleterious side effects due to increased RyR leak). Of the five tested hits, three – ebselen, disulfiram, and chloroxine –display a strong

correlation between alteration in FRET and RyR activity, as indicated by the correlation coefficient of the linear fit (Figure 6C). The apparently weak correlation in the effects of cefatrizine and tacrolimus may be due to a complex compound-RyR interaction, as suggested by the biphasic FRET response. In particular, the subtle effect of a change in RyR conformation would not be directly comparable to the larger FRET effect from dissociation of fluorescently labeled proteins (D-FKBP and A-CaM).

The detailed mechanism of hit action on the RyR complex is beyond the scope of this report. In this first pilot screen targeting RyR, the objective was simply to validate a method that can identify RyR modulators in HTS mode. Nevertheless, it is clear that the hits (1) affect [^{3}H]ryanodine binding in the absence of CaM, and (2) these effects are influenced by the presence of CaM. Since CaM itself is a modulator of RyR1 function (activator at nM [Ca^{2+}]; inhibitor at μM [Ca^{2+}]), we expected that a hit (which was identified due to its disruption of CaM binding) would affect RyR1 function in a CaM-dependent manner. Moreover, we might expect that a hit would affect the CaM-mediated modulation of [^{3}H]ryanodine binding by altering CaM-RyR1 binding. However, given the saturating [CaM] we used to test the impact of CaM on compound regulation of RyR1, this would only be apparent if a compound dramatically reduced CaM-RyR1 affinity – like disulfiram or ebselen – as indicated by FRET (Figure 4). In this instance, a shift in CaM binding might be reflected in a shift of RyR1 activity that is additive to the separate effect of the hit compound directly on the RyR. For example, if a hit directly activates RyR1 in low [Ca^{2+}] and also inhibits CaM binding to RyR1, we expect the overall functional effect to be impacted by a combination of the direct activating effect of the hit (that can be observed in the absence of CaM) and a reduced CaM-mediated RyR1 activation. This would then become apparent in the functional results as the activating effect of a compound being attenuated by the presence of CaM in low [Ca^{2+}]. This could easily be said for the effect of disulfiram (5–20 μM; Figure 5C) and ebselen (5–20 μM; Figure 5D) on RyR1 activity in the presence of CaM. Whereby, the putative drug-induced dissociation of CaM attenuates the activating effect of the drugs in 30 nM Ca^{2+} and enhances the effect of the drug in 30 μM Ca^{2+}, due to a reduction in CaM-mediated activation and inhibition at those respective [Ca^{2+}]. However, this model would not explain the CaM-dependent effects on other compounds that marginally alter FRET, given that this mode of action would likely be masked by the use of saturating [CaM] in [^{3}H]ryanodine binding assays. In the case of marginally significant modulators of FRET, the more plausible explanation is that CaM binding to RyR1 allosterically alters compound binding or its effect. This may be the case for at least cefatrizine (Figure 5B), tacrolimus (Figure 5E), and chloroxine (Figure 5F), but their actual mechanisms of action can only be determined through detailed studies beyond the scope of this report.

In summary, we have developed and validated an HTS platform designed to resolve small-molecule compounds that modulate RyR, laying the foundation for RyR-targeted HTS approaches to identify and develop agents that target RyR-mediated SR Ca^{2+} leak. In one screen of 727 compounds, we detected 5 modulators of RyR1 activity; two are known modulators, while three novel modulators were detected. To predict feasibility for identification of therapeutic agents that target RyR Ca^{2+} leak, one such compound may be a good candidate for further testing as a leak inhibitor *in situ*. With a screen of 20,000 compounds, as we previously carried out (34), we anticipate detecting ~150 novel effectors

of RyR, which would extensively expand our current knowledge of RyR1 pharmaco-modulation. Of these, we would expect ~30 small inhibitors of RyR as viable candidates to be used in secondary screens to validate their therapeutic potential for myopathies or neurological disorders.

Supplementary Material

Refer to Web version on PubMed Central for supplementary material.

Acknowledgments

This work was supported by American Heart Association Grant-in-Aid 15GRNT25610022 (to RLC) and Postdoctoral Fellowship [14POST20310024] (to RTR), NIH grants R01HL092097 (to RLC and DMB) and R37AG026160 (to DDT), and an STTR Phase II grant R42DA037622 (to GDG and DDT). The NCC assay plates were prepared by Samantha Yuen and Ji Li. Kurt Peterson, Ji Li provided helpful discussions for undertaking the HTS, and Octavian Cornea helped prepare the manuscript for publication. HTS was performed using the facilities provided by Fluorescence Innovations, Inc. (Minneapolis, MN, USA), with assistance from Kurt Peterson. Spectroscopy for dose-response assays was performed at the Biophysical Technology Center, Department of Biochemistry, Molecular Biology and Biophysics, University of Minnesota.

LITERATURE

1. Lanner JT. Ryanodine receptor physiology and its role in disease. Advances in experimental medicine and biology. 2012; 740:217–234. [PubMed: 22453944]
2. Liang L, Wei H. Dantrolene, a treatment for Alzheimer disease? Alzheimer disease and associated disorders. 2015; 29:1–5. [PubMed: 25551862]
3. Bers DM. Cardiac sarcoplasmic reticulum calcium leak: basis and roles in cardiac dysfunction. Annual review of physiology. 2014; 76:107–127.
4. Kho C, Lee A, Hajjar RJ. Altered sarcoplasmic reticulum calcium cycling--targets for heart failure therapy. Nature reviews. Cardiology. 2012; 9:717–733. [PubMed: 23090087]
5. Andersson DC, Betzenhauser MJ, Reiken S, Meli AC, Umanskaya A, Xie W, Shiomi T, Zalk R, Lacampagne A, Marks AR. Ryanodine receptor oxidation causes intracellular calcium leak and muscle weakness in aging. Cell metabolism. 2011; 14:196–207. [PubMed: 21803290]
6. McCauley MD, Wehrens XH. Targeting ryanodine receptors for anti-arrhythmic therapy. Acta pharmacologica Sinica. 2011; 32:749–757. [PubMed: 21642946]
7. Roe AT, Frisk M, Louch WE. Targeting cardiomyocyte Ca2+ homeostasis in heart failure. Current pharmaceutical design. 2015; 21:431–448. [PubMed: 25483944]
8. Van Petegem F. Ryanodine receptors: allosteric ion channel giants. Journal of molecular biology. 2015; 427:31–53. [PubMed: 25134758]
9. Andersson DC, Marks AR. Fixing ryanodine receptor Ca leak - a novel therapeutic strategy for contractile failure in heart and skeletal muscle. Drug discovery today. Disease mechanisms. 2010; 7:e151–e157. [PubMed: 21113427]
10. Aracena P, Tang W, Hamilton SL, Hidalgo C. Effects of S-glutathionylation and S-nitrosylation on calmodulin binding to triads and FKBP12 binding to type 1 calcium release channels. Antioxidants & redox signaling. 2005; 7:870–881. [PubMed: 15998242]
11. Oda T, Yang Y, Uchinoumi H, Thomas DD, Chen-Izu Y, Kato T, Yamamoto T, Yano M, Cornea RL, Bers DM. Oxidation of ryanodine receptor (RyR) and calmodulin enhance Ca release and pathologically alter, RyR structure and calmodulin affinity. Journal of molecular and cellular cardiology. 2015; 85:240–248. [PubMed: 26092277]
12. Uchinoumi H, Yang Y, Oda T, Li N, Alsina KM, Puglisi JL, Chen-Izu Y, Cornea RL, Wehrens XH, Bers DM. CaMKII-dependent phosphorylation of RyR2 promotes targetable pathological RyR2 conformational shift. Journal of molecular and cellular cardiology. 2016; 98:62–72. [PubMed: 27318036]

13. Oda T, Yang Y, Nitu FR, Svensson B, Lu X, Fruen BR, Cornea RL, Bers DM. In cardiomyocytes, binding of unzipping peptide activates ryanodine receptor 2 and reciprocally inhibits calmodulin binding. Circulation research. 2013; 112:487–497. [PubMed: 23233753]
14. Yang Y, Guo T, Oda T, Chakraborty A, Chen L, Uchinoumi H, Knowlton AA, Fruen BR, Cornea RL, Meissner G, Bers DM. Cardiac myocyte Z-line calmodulin is mainly RyR2-bound, and reduction is arrhythmogenic and occurs in heart failure. Circulation research. 2014; 114:295–306. [PubMed: 24186966]
15. Blayney LM, Jones JL, Griffiths J, Lai FA. A mechanism of ryanodine receptor modulation by FKBP12/12.6, protein kinase A, and K201. Cardiovascular research. 2010; 85:68–78. [PubMed: 19661110]
16. Yan Z, Bai XC, Yan C, Wu J, Li Z, Xie T, Peng W, Yin CC, Li X, Scheres SH, Shi Y, Yan N. Structure of the rabbit ryanodine receptor RyR1 at near-atomic resolution. Nature. 2015; 517:50–55. [PubMed: 25517095]
17. Cornea RL, Nitu F, Gruber S, Kohler K, Satzer M, Thomas DD, Fruen BR. FRET-based mapping of calmodulin bound to the RyR1 Ca2+ release channel. Proc Natl Acad Sci U S A. 2009; 106:6128–6133. [PubMed: 19332786]
18. Cornea RL, Nitu FR, Samso M, Thomas DD, Fruen BR. Mapping the ryanodine receptor FK506-binding protein subunit using fluorescence resonance energy transfer. J Biol Chem. 2010; 285:19219–19226. [PubMed: 20404344]
19. Gruber SJ, Cornea RL, Li J, Peterson KC, Schaaf TM, Gillispie GD, Dahl R, Zsebo KM, Robia SL, Thomas DD. Discovery of enzyme modulators via high-throughput time-resolved FRET in living cells. Journal of biomolecular screening. 2014; 19:215–222. [PubMed: 24436077]
20. Petersen KJ, Peterson KC, Muretta JM, Higgins SE, Gillispie GD, Thomas DD. Fluorescence lifetime plate reader: resolution and precision meet high-throughput. The Review of scientific instruments. 2014; 85:113101. [PubMed: 25430092]
21. Fruen BR, Bardy JM, Byrem TM, Strasburg GM, Louis CF. Differential Ca(2+) sensitivity of skeletal and cardiac muscle ryanodine receptors in the presence of calmodulin. American journal of physiology. Cell physiology. 2000; 279:C724–733. [PubMed: 10942723]
22. Fruen BR, Black DJ, Bloomquist RA, Bardy JM, Johnson JD, Louis CF, Balog EM. Regulation of the RYR1 and RYR2 Ca2+ release channel isoforms by Ca2+-insensitive mutants of calmodulin. Biochemistry. 2003; 42:2740–2747. [PubMed: 12614169]
23. Fruen BR, Balog EM, Schafer J, Nitu FR, Thomas DD, Cornea RL. Direct detection of calmodulin tuning by ryanodine receptor channel targets using a ca(2+)-sensitive acrylodan-labeled calmodulin. Biochemistry. 2005; 44:278–284. [PubMed: 15628869]
24. Muretta JM, Kyrychenko A, Ladokhin AS, Kast D, Gillispie GE, Thomas DD. High -performance time-resolved fluorescence by direct waveform recording. Rev Sci Instrum. 2010; 81:103101–103108. [PubMed: 21034069]
25. Zhang JH, Chung TD, Oldenburg KR. A Simple Statistical Parameter for Use in Evaluation and Validation of High Throughput Screening Assays. J Biomol Screen. 1999; 4:67–73. [PubMed: 10838414]
26. Mazurek SR, Bovo E, Zima AV. Regulation of sarcoplasmic reticulum Ca(2+) release by cytosolic glutathione in rabbit ventricular myocytes. Free radical biology & medicine. 2014; 68:159–167. [PubMed: 24334252]
27. Meissner G, Pasek DA, Yamaguchi N, Ramachandran S, Dokholyan NV, Tripathy A. Thermodynamics of calmodulin binding to cardiac and skeletal muscle ryanodine receptor ion channels. Proteins. 2009; 74:207–211. [PubMed: 18618700]
28. Hughes JP, Rees S, Kalindjian SB, Philpott KL. Principles of early drug discovery. British journal of pharmacology. 2011; 162:1239–1249. [PubMed: 21091654]
29. MacMillan D. FK506 binding proteins: cellular regulators of intracellular Ca2+ signalling. European journal of pharmacology. 2013; 700:181–193. [PubMed: 23305836]
30. Xia R, Ganther HE, Egge A, Abramson JJ. Selenium compounds modulate the calcium release channel/ryanodine receptor of rabbit skeletal muscle by oxidizing functional thiols. Biochemical pharmacology. 2004; 67:2071–2079. [PubMed: 15135304]

31. Fruen BR, Mickelson JR, Louis CF. Dantrolene inhibition of sarcoplasmic reticulum Ca2+ release by direct and specific action at skeletal muscle ryanodine receptors. The Journal of biological chemistry. 1997; 272:26965–26971. [PubMed: 9341133]

32. Joumaa WH, Bouhlel A, Leoty C. Effects of disulfiram on excitation-contraction coupling in rat soleus muscle. Naunyn-Schmiedeberg's archives of pharmacology. 2003; 368:247–255.

33. Cully TR, Launikonis BS. Leaky ryanodine receptors delay the activation of store overload-induced Ca2+ release, a mechanism underlying malignant hyperthermia-like events in dystrophic muscle. Am J Physiol Cell Physiol. 2016; 310:C673–680. [PubMed: 26825125]

34. Cornea RL, Gruber SJ, Lockamy EL, Muretta JM, Jin D, Chen J, Dahl R, Bartfai T, Zsebo KM, Gillispie GD, Thomas DD. High-throughput FRET assay yields allosteric SERCA activators. J Biomol Screen. 2013; 18:97–107. [PubMed: 22923787]

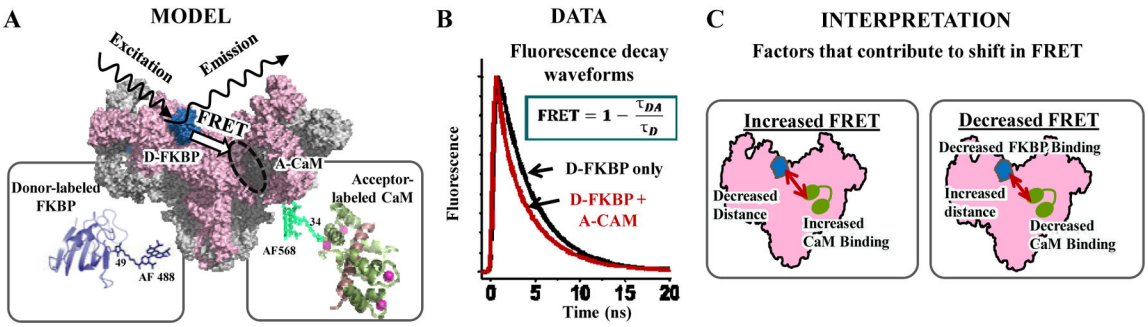

Figure 1. FRET-based HTS-compatible system to monitor RyR interaction with CaM and FKBP

(A) Schematic illustration of the FKBP and CaM binding locations within the RyR cryo-EM map (16,17), and donor and acceptor label positions on ribbon-structures of FKBP and CaM, respectively (PDB 4IQ2 and 2BCX). (B) Time-resolved (TR) fluorescence waveforms yield the fluorescence lifetime (FLT) readout that enables high-precision measurements of FRET between D-FKBP and A-CaM. FRET is calculated as the fractional change between the fluorescence lifetimes of donor-only and donor+acceptor sample lifetime (τ_D and τ_{DA}, respectively). (C) FRET changes can be due to alterations in FKBP or CaM binding affinity and/or RyR structure that affects distance relationships between fluorophores.

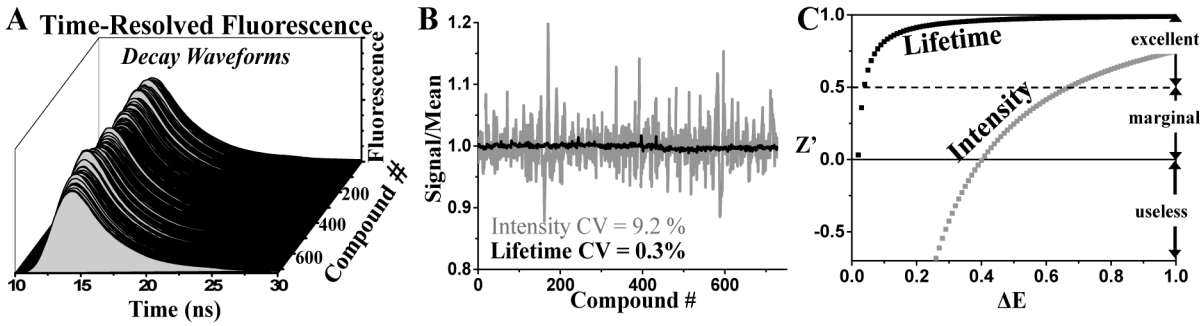

Figure 2. Performance of time-resolved fluorescence properties: lifetime vs. peak intensity

(A) Time-resolved fluorescence waveforms from RyR-targeted, FRET-based HTS of NCC library (10 μM test-compounds) performed in 384-well format. (B) The lifetime measurement affords ~30× higher precision than intensity detection. (C) The relationship between the HTS assay quality, Z′, and the signal window, ΔE, indicates that fluorescence lifetime enables excellent quality even for minuscule ΔE (of ≥0.03), relative to the fluorescence intensity, which requires a much larger ΔE (of >0.6) for the same quality. All fluorescent compounds that interfere with donor probe lifetime were removed from the data set.

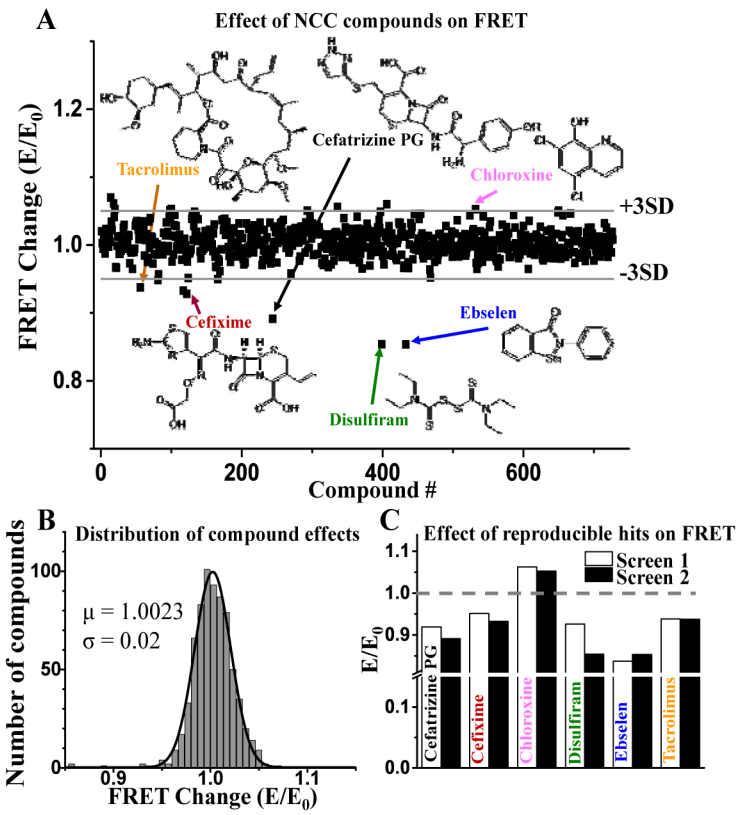

Figure 3. HTS results

A FRET screen of NCC library (727 compounds, 10 μM) to detect modulators of RyR/FKBP/CaM complex was undertaken in duplicate. FRET of donor-labeled FKBP (D-FKBP) by acceptor-labeled CaM (A-CaM) was calculated from donor fluorescence lifetime. Then FRET for each compound (E) was normalized to DMSO control (E_0). (A) Normalized FRET from one screen with hit threshold (>3SD of mean) indicated by grey lines. Reproducible hit compounds and their chemical structure are indicated by arrows. (B) Gaussian fit of the E/E_0 distribution. (C) Normalized effects (E/E_0) of hits identified in two separate screens.

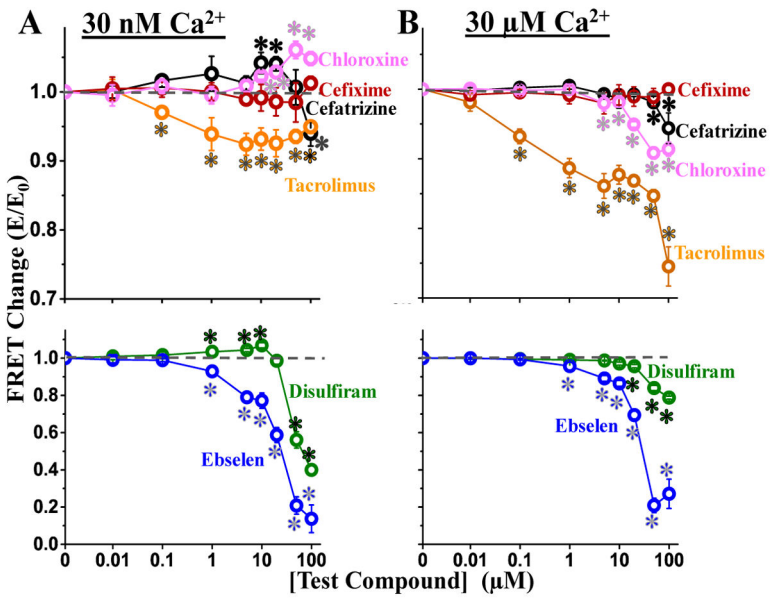

Figure 4.

Dose-response of screen Hits on FRET at 30 nM Ca^{2+} (A) and 30 µM Ca^{2+} (B). Symbols indicate FRET mean ± SE for chloroxine (pink), cefixime (red), cefatrizine PG (black) and Tacrolimus (orange) in the upper panels, and disulfiram (green) and ebselen (blue) in the lower panels. *Significantly different from the DMSO-only control using unpaired Student's t-test, $p > 0.05$.

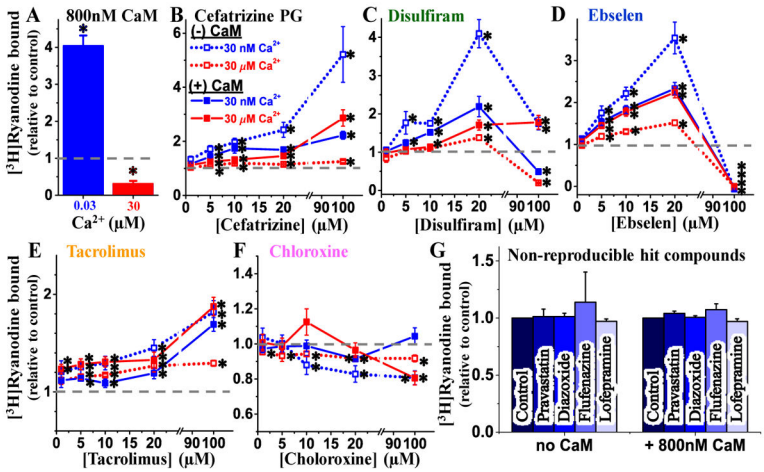

Figure 5.

[^{3}H]Ryanodine binding assays to determine the dose-dependent effect of hits on the RyR1 function. (A) In control experiments, HSR vesicles were incubated with 0 or 800 nM CaM in the presence of [^{3}H]ryanodine, at 30 nM and 30 μM free Ca^{2+}. Results are shown normalized relative to the values for (−)CaM controls. (B–F) Dose dependent (0–100 μM) effect of screen Hit compounds on [^{3}H]ryanodine binding to skeletal SR membranes when incubated in the absence of CaM (*open symbol*) or in the presence of 800 nM CaM (*solid symbol*), at 30 nM (*blue*) and 30 μM (*red*) free Ca^{2+}. Results are shown normalized relative to the values for no-drug control (dashed line), mean ±SE, n = 6–10. (G) Effect of 10 μM non-reproducible hit compounds from screen on [^{3}H]ryanodine binding to skeletal SR membranes when incubated in absence or presence of 800 nM CaM at 30 nM Ca^{2+}. *Significantly different from control (DMSO only) using unpaired Student's t-test, p> 0.05.

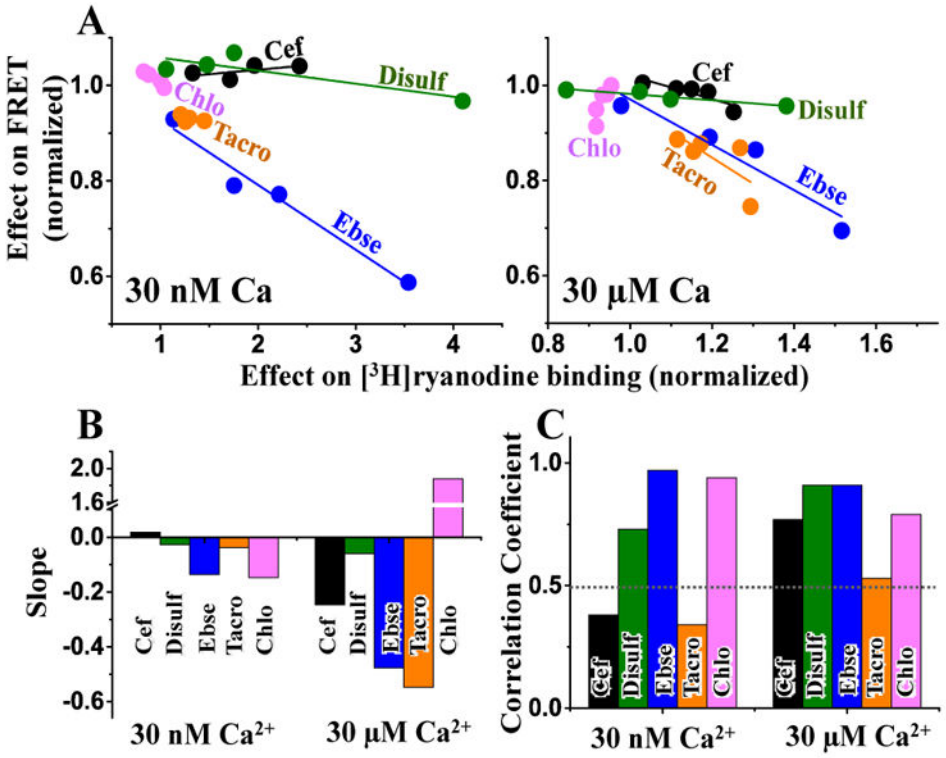

Figure 6.

Correlation between hit effects on FRET and RyR1 activity. (A) The change in mean FRET is plotted versus the change in mean [^{3}H]ryanodine binding to skeletal SR membranes in low Ca^{2+} (30 nM, left panel) and high Ca^{2+} (30 µM, right panel), in the absence of CaM. The effects are plotted relative to the no-drug control. Only the effects of compound concentration within pharmacological range (≤ 20 µM from Figure 4 and Figure 5) were included in this analysis. Fitting parameters from panel A are shown as slope (B) and correlation coefficient (C)